Design of an Energy Harvester

ME 128 – Project 3c

Professor Liwei Lin
Spring 2006

Scott Moura
SID 15905638

May 15, 2006

ME128 – Computer-Aided Mechanical Design

Spring 2006

Name: **Scott** **Moura**

Project: **#3c Design of an Energy Harvester**

Introduction:	10	_____
Theory/Approach:	20	_____
Result Verification:	10	_____
Results:	20	_____
FEM Results:	10	_____
Discussions and Conclusions:	20	_____
Appendix (source code …):	10	_____
Total:	100	_____

May 15, 2006

Table of Contents

Introduction

Micro-power generation systems have gained considerable research attention due to the rapid development of micro-electromechanical systems and wireless technologies. To this day batteries serve as the most common power source for remote wireless systems. However, these power systems have grown impractical for large networks and small devices, where replacing depleted batteries becomes difficult. Therefore, alternative solutions characterized by a renewable power supply of reasonable power density have been suggested.

High frequency vibrations offer a plausible source of energy for conversion into usable electrical power. In this project, we wish to investigate a piezoelectric micro-power generator designed to operate in a high frequency environment. A piezoelectric-based power generation system has been chosen since it generates the highest power output for a given size, relative to other energy converters [1]. Our goal is to design an energy harvester capable of producing 2.5mW without exceeding various geometric and mechanical constraints.

Due to the complex nature of the problem, a genetic algorithm (GA) id developed for optimization. The GA attempts to either maximize output power or decrease total volume while satisfying all other engineering goals. Seven dimensions (L, b, t, h, x_m, y_m, z_m) are determined from this optimization. The optimal design from the theoretically derived genetic algorithm is compared to finite element analysis (FEA) in order to ascertain its accuracy and verify the results.

The genetic algorithm, developed in MATLAB, utilizes concepts from evolution in order to ascertain the best performing design. Although computationally intense, this method is very useful for complex problems in which systems of differential equations are difficult to write. Since optimization methods are not the focus of this project, details about how genetic algorithms work are omitted.

The software used for finite element analysis (FEA) is SolidWorks with the built-in COSMOSWorks finite element method (FEM) analysis package. Three-dimensional models of two proposed designs are created and analyzed using

both frequency and static analyses. Each simulation represents the limiting conditions of operation, and are therefore of interest for evaluating the maximum power output, stress, deflection, and natural frequency.

Theory/Approach

Simple beam bending combined with a theoretical model developed by Lu *et al* provides the theoretical approach to optimize the design of a piezoelectric generator. This approach is chosen for its simplicity in terms of requiring no in-depth piezoelectric material analysis. Additionally, simple finite element models can be constructed and analyzed to provide a general direction for more in-depth analyses.

Beam Bending Analysis

To model the deformation of the piezoelectric cantilever design, an elastic cantilever beam under a concentrated load is considered. This model assumes a single isentropic material, even though the actual structure consists of a piezoelectric bimorph. A schematic of the system is shown in Figure 1.

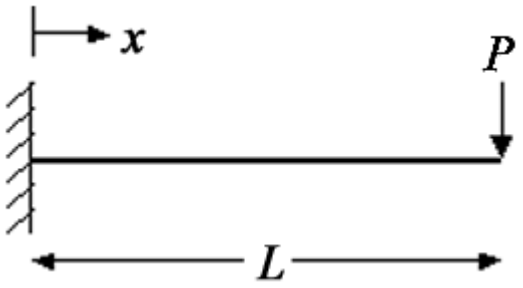

Figure 1: Elastic cantilever beam under a concentrated load at the end.

The governing differential equations for elastic beam bending serve as the basis for the theoretical beam analysis. They are given below:

$$EI\frac{d^2u}{dx^2} = M(x) \qquad \text{Moment} \qquad (1)$$

$$\frac{du}{dx} = \theta(x) \qquad \text{Angle of Deflection} \qquad (2)$$

$$u = u(x) \qquad \text{Deflection} \qquad (3)$$

These equations assume a perfectly elastic beam with small deflections. Additionally, the beam is modeled as a two-dimensional curve to simplify the derivations.

$$M(x) = EI\frac{d^2u}{dx^2} = P(x-L) \tag{4}$$

$$\theta(x) = \frac{du}{dx} = \frac{P}{2EI}(x-L)^2 + C_1 \tag{5}$$

$$u(x) = \frac{P}{6EI}(x-L)^3 + C_1x + C_2 \tag{6}$$

The following boundary conditions, prescribed by the fixed end of a cantilever, are used to evaluate the constants of integration.

Boundary Conditions

$$y(x=0) = 0 \tag{7}$$

$$\theta(x=0) = 0 \tag{8}$$

Algebraic manipulation gives the following values for the constants of integration:

Integration Constants

$$C_1 = -\frac{PL^2}{2EI} \tag{9}$$

$$C_2 = \frac{PL^3}{6EI} \tag{10}$$

As a result, the following governing equations provide the displacement and angle of displacement as functions of x.

Governing Equations

$$\theta(x) = \frac{P}{2EI}(x-L)^2 - \frac{PL^2}{2EI} \tag{11}$$

$$u(x) = \frac{P}{6EI}(x-L)^3 - \frac{PL^2}{2EI}x + \frac{PL^3}{6EI} \tag{12}$$

Piezoelectric Power Generation

The vibration-to-electricity energy converter is described by a two-layer bending element (bimorph) mounted as a cantilever beam with a proof mass placed at the free end, as shown in Figure 2. This system provides the highest average strain per force input, which consequently produces the highest average power output. Additionally, a cantilever system can be characterized by resonant frequencies in the range of the target frequency (100 to 200 Hz) [1].

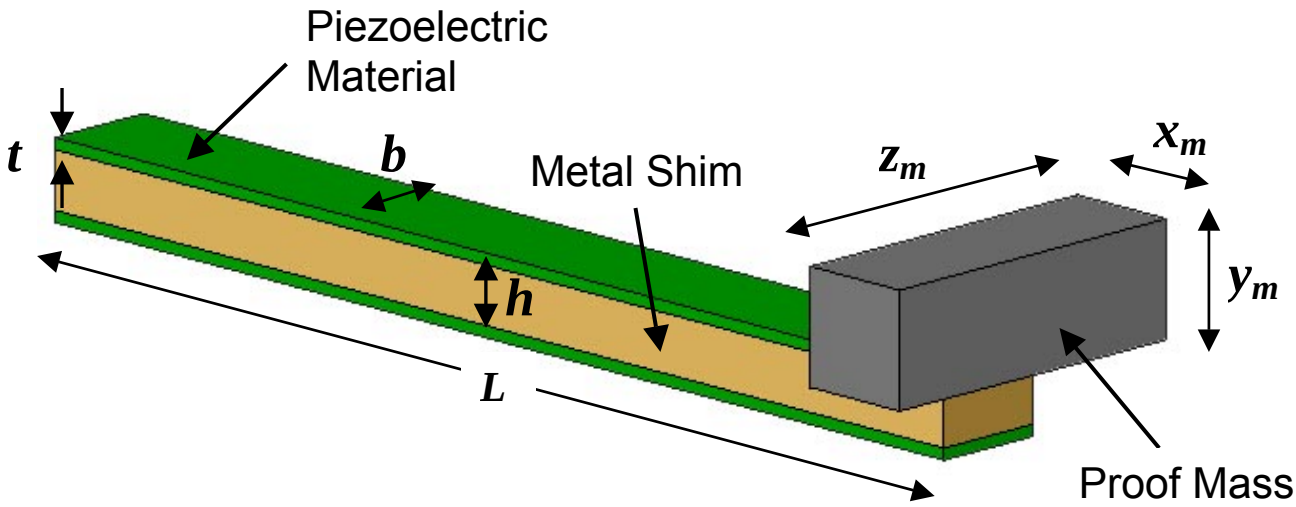

Figure 2: Piezoelectric power generator with a bimorph-cantilever design. The proof mass is added to adjust the resonant frequency and maximum strain. *L* is the beam length, *b* is the beam width, *t* is the piezoelectric material thickness, *h* is the metal shim thickness, and x_m, y_m, z_m are the dimensions of the proof mass.

In order to produce the maximum deformation of the piezoelectric material and consequently the most power, it is assumed that the generator operates at the resonant frequency of the vibrating structure. The resonant frequency is found by combining Newton's Second Law and Hooke's Law (Equation 13).

$$\omega = \sqrt{\frac{k}{m}} = \sqrt{\frac{ma}{u}\cdot\frac{1}{m}} = \sqrt{\frac{a}{u}} = \sqrt{\frac{Ebh^3}{4\rho x_m y_m z_m L^3}} \tag{13}$$

To produce any electrical power, a resistive load is required. For simplification, the electrical load is modeled as a single resistor. Simple circuit analysis shows that the power generated is a function of the matching resistance. Therefore, an optimum resistance can be found to produce maximum power. Lu *et al* suggests the output power reaches its maximum value when the resistance is described by Equation 14. In reality, the electronics connected to the power generator would consist of more than just one resistor. However, a detailed analysis of these electronics is beyond the scope of this project.

$$R = \frac{t}{bL\varepsilon_{33}\omega} \tag{14}$$

According to Lu *et al*, the time-averaged power generated by a bimorph piezoelectric cantilever design is modeled by Equation 15, where b is the width of the beam, h is the height of the metal shim, A is the angle of displacement, L is the beam length, and t is the thickness of the piezoelectric layer. From this

equation, it is found that the output power is dependent on the excitation frequency, ω, and the external resistance, R. For maximum power, the natural frequency of the structure, described by Equation 13, is used for ω and Equation 14 is used for R.

$$Power = \frac{\omega^2 b^2 h^2 e_{31}{}^2 A^2}{4\left(1 + bL\varepsilon_{33}\frac{\omega R}{t}\right)^2} R \tag{15}$$

Consider L, b, t, h, x_m, y_m, z_m as the seven design variables to be used in the optimization process. Substituting Equations 11-14 into 15 and applying the beam bending analysis produces the following expression for power that can be written in terms of only design variables and constants:

$$Power = \frac{9\rho^{3/2} e_{31}{}^2 a^2}{8E^{3/2}\varepsilon_{33}} \cdot \frac{L^{3/2} t x_m{}^{3/2} y_m{}^{3/2} z_m{}^{3/2}}{h^{5/2} b^{1/2}} \tag{16}$$

Cleary, increasing the length of the beam and the dimensions of the proof mass will increase power output. However, these values are limited by geometric and material constraints. Equation 16 also reveals that minimizing the beam thickness will increase power. Therefore we expect all designs to have small beam widths. A final observation of interest is that power increases when the piezoelectric material thickness is large and metal shim thickness is small. However, this model was developed under the assumption that the piezoelectric material thickness is much smaller than the shim thickness. Therefore these parameters must conform to this assumption. Note that this model has also been developed under the assumption that the piezoelectric material does not have a significant effect on the flexibility of the metal shim. It is critical that these assumptions agree with any suggested design in order to utilize the model proposed by Lu *et al*. If it is impossible to create a successful design that satisfies these assumptions, new design configurations should be investigated.

Engineering Constraints & Goals

Coupled with the theoretical model provided above, a successful design must satisfy the following engineering constraints:

Maximum volume of device: $VOLUME_{\max} \leq 50{,}000mm^3$ (17)

Maximum Cross Sectional Area (viewing from the top): $AREA_{\max} \leq 2{,}500mm^2$ (18)

Acceleration of vibration source: $a \leq 0.2g$ (19)

Thickness of piezo-layer: $0.1mm \leq t \leq 1mm$ (20)

Thickness of metal shim: $0.1mm \leq h \leq 1mm$ (21)

Width of beam: $b \geq 1mm$ (22)

These parameters are requirements determined by the manufacturing process, size restrictions, and application environment. Within these constraints, this investigation seeks to accomplish three engineering goals outlined by the following descriptions:

Minimum power output: $Power \geq 2.5mW$ (23)

Maximum allowable stress in PZT: $\sigma_{max} \leq 25MPa$ (24)

Natural frequency of the harvester: $100Hz \leq f \leq 200Hz$ (25)

Code Verification

The genetic algorithm written in MATLAB is compared to hand-derived calculations to prove the accuracy of the code. For verification purposes, the seven design variables are given a value of 1. This makes for easy hand calculations, if not particularly useful towards achieving the goals of this project. The results for the most significant energy harvester properties are shown in Table 1. These values match perfectly, thus ensuring the program's precision.

Table 1: Code Verification Table.

	Output Power	Maximum Stress	Natural Frequency	Total Volume	Resistance for Max Power
MATLAB Calculations	4.1482 mW	25,153 Pa	1019.4 Hz	1.5 m^3	5040.3 Ω
Hand Calculations	4.15 mW	25,000 Pa	1020 Hz	1.5 m^3	5040 Ω

Results

The genetic algorithm developed for this investigation finds the optimum design based on two different criteria. The first (Design #1) maximizes output power

while satisfying all the other design constraints. The second (Design #2) minimizes total volume. The results are given in Tables 2 and 3.

Table 2: Results of the Genetic Algorithm Optimization Method. Design #1 maximizes power, Design #2 minimizes volume.

Design Parameter	Design #1 Value	Design #2 Value
L	13.531 mm	17.074 mm
b	18.595 mm	29.079 mm
t	0.1 mm	0.1 mm
h	1 mm	1 mm
x_m	26.920 mm	33.997 mm
y_m	54.623 mm	18.821 mm
z_m	33.904 mm	59.664 mm

Table 3: Energy Harvester Properties for optimum designs found by GA. Design #1 maximizes power, Design #2 minimizes volume.

Energy Harvester Property	Design #1 Value	Design #2 Value
Power	3.29183 mW	2.5 mW
Natural Frequency	100.0673 Hz	100.8855 Hz
Maximum Stress	5.7031 MPa	3.5239 MPa
Cross-Sectional Area (Top View)	915 mm^2	2,033 mm^2
Volume of Device	49,995 mm^3	38,281 mm^3
Matching Resistance	20.408 kΩ	10.258 kΩ
Maximum Displacement	4.9581 μm	4.878 μm
Maximum Angle of Displacement	-0.0315°	-0.0246°

Matching Resistance and Driving Frequency

For any typical application, a resistive load is required to produce power. This fact is reflected by Equation 15, in which power is clearly seen as a function of resistance. Moreover, Equation 15 reveals that the driving frequency also influences power output. Ideally, the energy harvester must operate at the natural frequency to take advantage of resonance. In addition, a matching resistance equivalent to that defined by Equation 14 theoretically produces the

most power. Nonetheless, it is of interest to understand how both the external resistance and driving frequency impact power output.

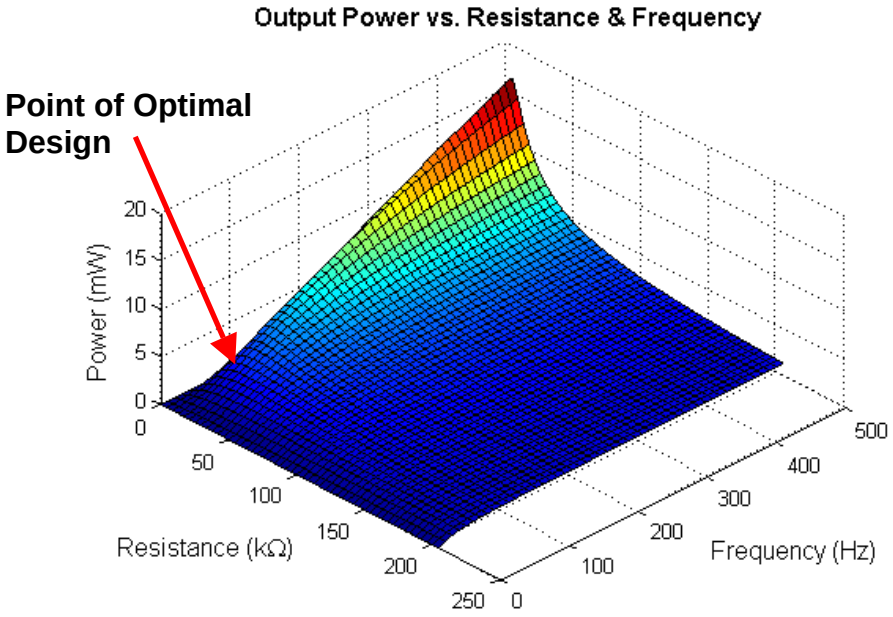

Figure 3: Output power as functions of both external resistance and frequency for Design #1 obtained from the genetic algorithm.

Figure 3 reveals that power increases when frequency increases and resistance decreases. This observation is confirmed by examining Equation 15, in which power is directly related to frequency and inversely related to resistance. However, the constraints imposed by the application environment require a natural frequency between 100 and 200Hz, thereby limiting the power output. With this limited range in mind, it appears that a design with a natural frequency of 200 Hz would produce the most power. Figure 3 may support this assertion, however the maximum allowable volume of the device cannot be surpassed. As a result, the optimal design found by the genetic algorithm maintains a natural frequency of about 100 Hz. These trends are true for both designs. A cross-section of Figure 3 detailing power output for Design #1 as a function of frequency is shown in Figure 4. This plot uses the external resistance value for maximum power output, given by Equation 14. Design #2 produces a similar plot.

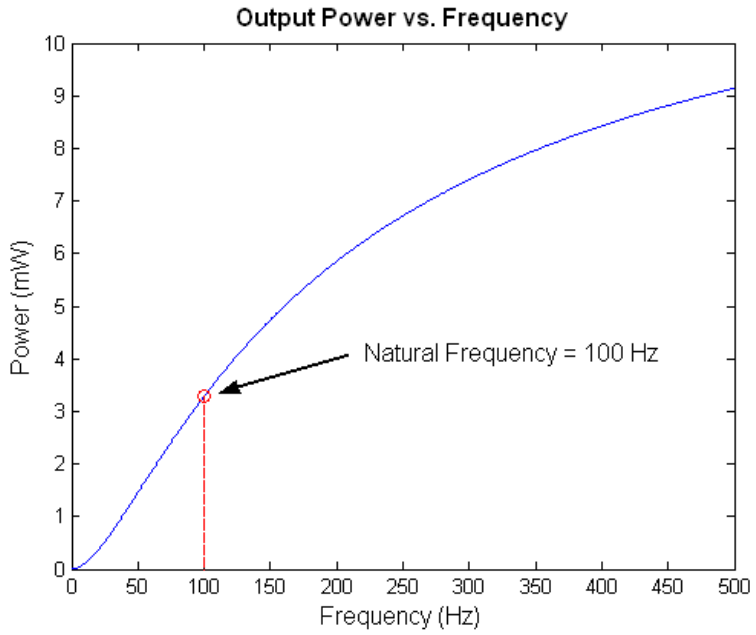

Figure 4: Output power as a function of operating frequency for Design #1. The external resistance value is prescribed by Equation 14.

The relationship between external resistance and output power for Design #1 is shown in Figure 5 for a driving frequency equal to the natural frequency. As expected, maximum power occurs when the resistance is defined by Equation 14. This resistance is equal to 20.408 kΩ for Design #1 and 10.258 kΩ for Design #2.

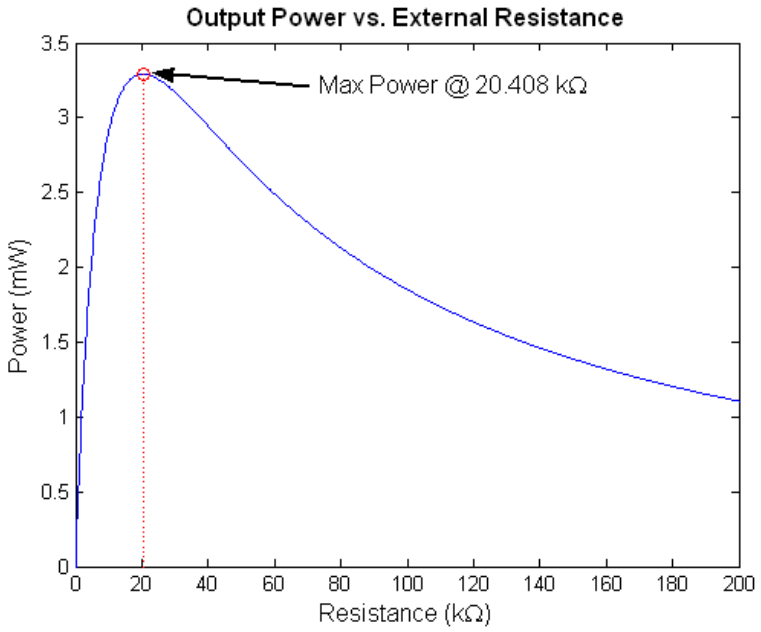

Figure 5: Output power as a function of external resistance. The driving frequency is equal to the natural frequency of the system.

Project Goals & Metrics

The optimal designs found through genetic optimization satisfy all the given design goals. Table 4 summaries these design goals and metrics. Two designs are recommended in this project. Design #1 seeks to maximize the output power of the energy harvester by utilizing the maximum amount of volume. Design #2 makes exactly 2.5 mW of power but attempts to minimize the overall volume of the device. The final results are two designs that both satisfy the constraints and engineering goals and can be utilized for different purposes, depending on the application.

Table 4: Design Goal Metric Table. The green shading indicates the optimal design satisfies the corresponding design goal.

Design Goals	Design #1	Design #2
$Power \geq 2.5mW$	**3.29183 mW**	**2.5 mW**
$\sigma_{max} \leq 25MPa$	**5.7031 MPa**	**3.5239 MPa**
$100Hz \leq f \leq 200Hz$	**100.0673 Hz**	**100.8855 Hz**
$VOLUME_{\max} \leq 50{,}000mm^3$	**49,995 mm^2**	**38,281 mm^3**

FEM Results

SolidWorks Modeling and Simulation

The finite element analysis was performed within SolidWorks using the COSMOSWorks package. This program allows the user to select a custom material for each part by inputting user-defined values for the material properties. The instructor provides the material properties used for this analysis. However, as discussed previously, tungsten is used in place of ABS plastic due to its relatively high density. Table 5 summaries all of the pertinent material properties:

Table 5: Summary of material properties used for finite element analysis.

Material	Elastic Modulus (E)	Poisson's Ratio (ν)	Mass Density (ρ)
Copper metal shim	$11.7\times10^{10}\,N/m^2$	0.34	$8900kg/m^3$
Piezoelectric layer	$6.3\times10^{10}\,N/m^2$	0.31	$7800kg/m^3$
Tungsten proof mass	$3.45\times10^{11}\,N/m^2$	0.28	$19250kg/m^3$

Figure 6 shows the SolidWorks model of Designs #1 and #2 developed under the optimized design parameters. The copper metal shim is shown in gold, the piezoelectric layers are shown in green, and the proof mass is shown in gray. At first sight it is evident that the proof mass is massive in relation to the bender. This will have a significant effect on the moment of inertia and natural frequency, to be discussed later.

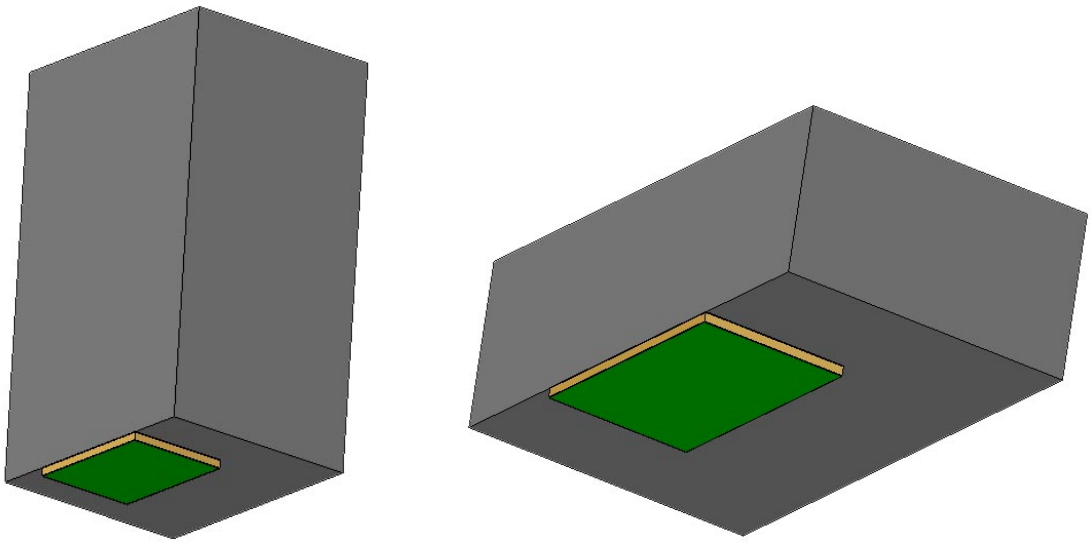

(a) **(b)**

Figure 6: SolidWorks models Designs #1 and #2. The copper metal shim is shown in gold, the piezoelectric layers are shown in green, and the proof mass is shown in gray.

The enormous proportions of the proof mass relative to the piezoelectric layers create issues in meshing the entire model. The global mesh size must be less than 0.1mm in order to accurately analyze the piezoelectric layers. However, SolidWorks is not capable of producing enough 0.1mm elements to mesh the entire model. As a result, an alternative technique was used on both designs to run the analyses. The alternative technique uses a 4mm x 4mm x b proof mass to simulate the actual proof mass, where b is the width of the beam. In this case, the force induced on the bender is made equivalent to the actual designs by adjusting the mass density of the proof mass. This allows SolidWorks to successfully mesh the models. A visual example is provided in Figure 7.

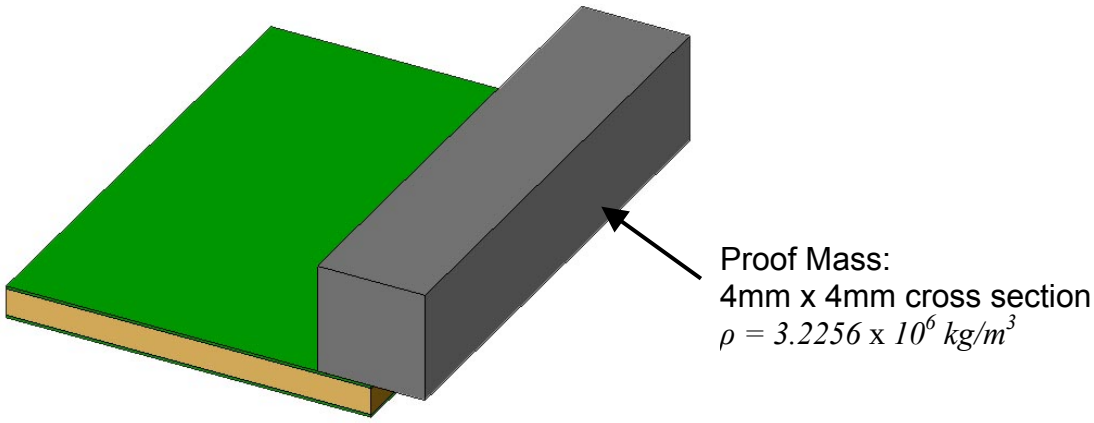

Figure 7: Alternative design used to simulate Design #1.

Two analyses are performed to validate the theoretical models. The first includes a frequency analysis to determine the natural frequency of the cantilever-proof mass system. The second is a static analysis to determine displacement, angle of displacement, and stress. All of the results are summarized in Table 6:

Table 6: Summary of FEA results on the optimized designs. Results obtained from both frequency and static analyses.

FEA Results	Design #1	Design #2
Natural Frequency	89.215 Hz	92.029 Hz
Maximum Stress	4.348 MPa	2.712 MPa
Maximum Displacement	5.577 μm	6.790 μm
Maximum Angle of Displacement	-0.0351°	-0.0275°

Design #1 – Maximum Power

The figures provided below portray the FEM calculations performed in COSMOS using SolidWorks. In all, three plots were analyzed to obtain the results given above. They include the first frequency mode, the stress distribution under a vibratory acceleration of 0.2g, and the maximum displacement.

Natural Frequency

The first frequency mode represents the one of most interest. As shown below, the natural frequency for Design #1 is 89.215 Hz according to the FEA. This agrees reasonably well with the theoretical value of 100 Hz.

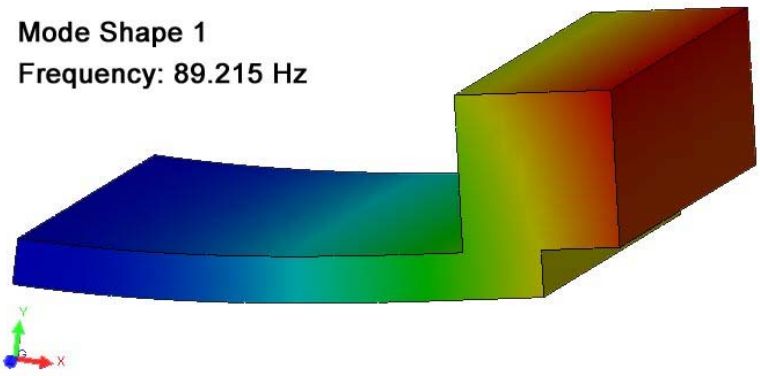

Figure 8: Mode Shape 1 for Design #1 using frequency FEA.

Maximum Stress

According to the theory developed previously, it is expected that the maximum stress is located at the fixed end. Figure 9 confirms this assertion and states the maximum stress is 4.349 MPa. This value is relatively close to the theoretically derived value of 5.7031 MPa.

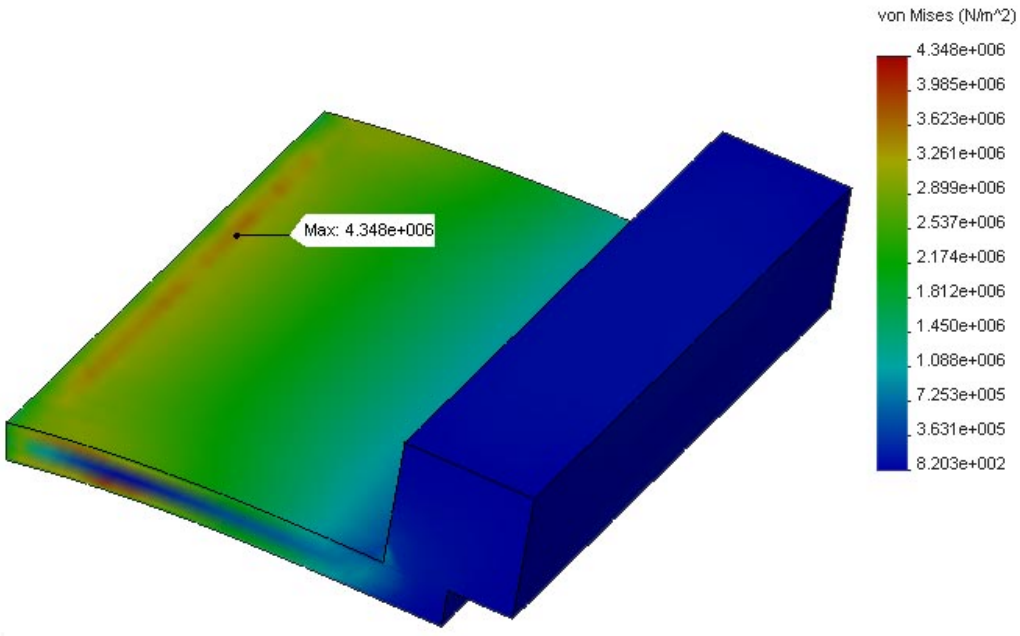

Figure 9: Stress Distribution for Design #1 using static FEA.

Maximum Displacement

Intuitively, the displacement should increase to a maximum in the x-direction. Figure 10 confirms this hypothesis. Although the maximum displacement is not exactly the value determined theoretically, it is within one order of magnitude and therefore considered reasonably accurate. It should be noted that the

displacement taken is at the free end of the beam, not the corner of the proof mass.

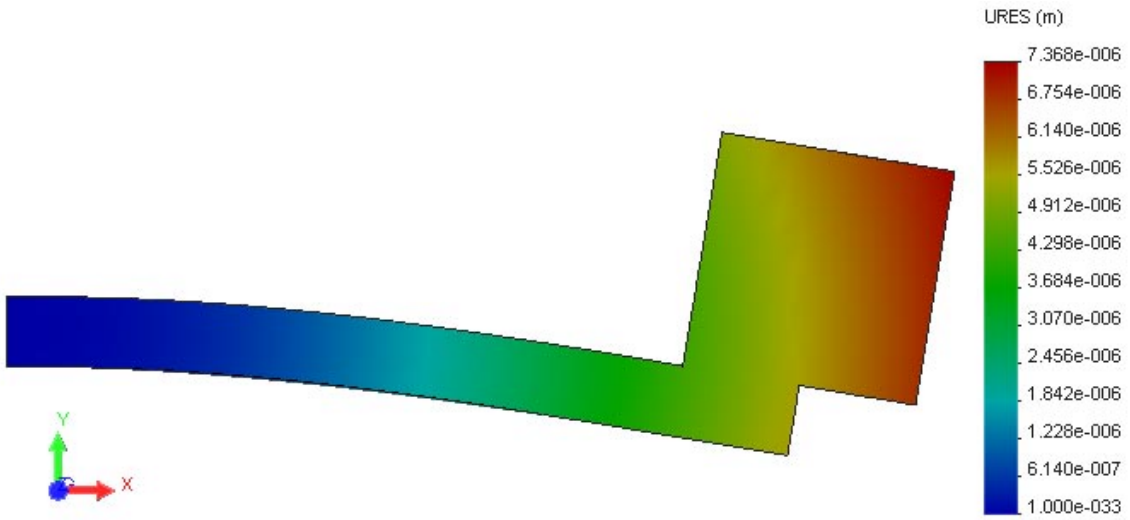

Figure 10: Maximum displacement for Design #1 under 0.2g of acceleration.

Design #2 – Minimum Volume

Natural Frequency

FEA on Design #2 gives a natural frequency of 92.029 Hz for the first vibration node. It is interesting that Design #2 deforms in the opposite direction as Design #1 for this frequency analysis. However, this outcome is inconsequential to the results of the report.

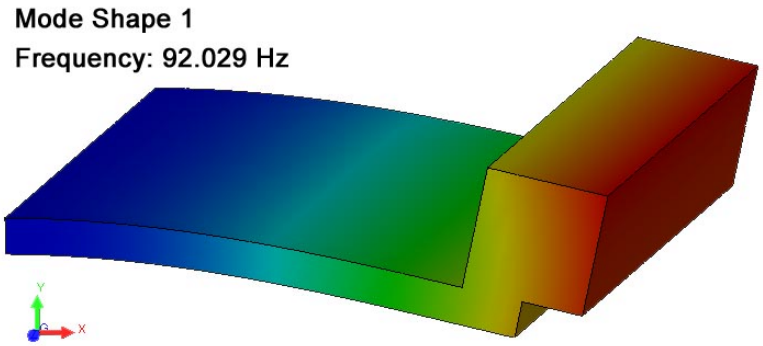

Figure 11: Mode Shape 1 for Design #2 using frequency FEA.

Maximum Stress

According to the FEA, the maximum stress also occurs near the fixed end of Design #2. Moreover, the value of maximum stress agrees well with the theoretical value.

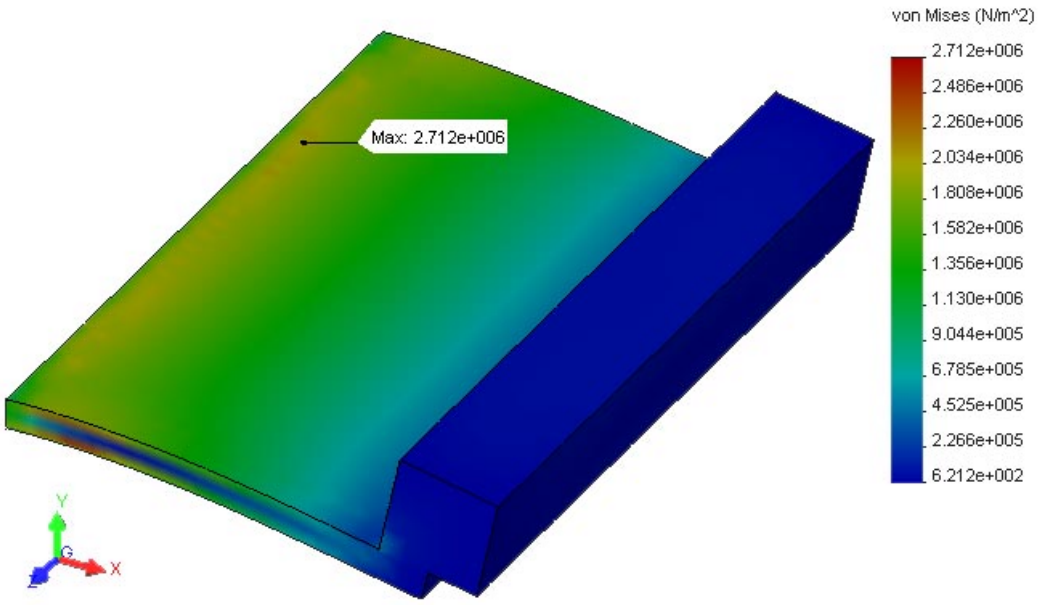

Figure 12: Stress Distribution for Design #2 using static FEA.

Maximum Displacement

Design #2 is submitted to an acceleration of 0.2g to produce the displacement plot shown below. The maximum displacement is 5.461 μm.

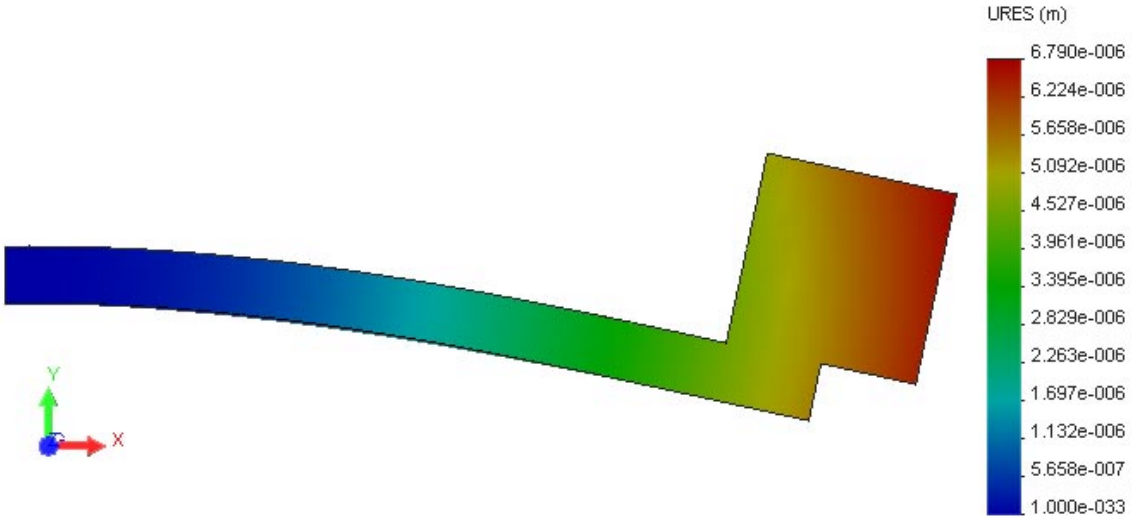

Discussion and Conclusions

Theoretical Considerations

A simplified analytical model provided in the project description estimates the power generated from a piezoelectric energy harvester, given by Equation 15. However, the project description erroneously claims that variable A is equal to the maximum beam deflection. Simple dimensional analysis reveals that this is not

true and A must be dimensionless. To determine the true meaning of A requires careful reading and understanding of a paper by Lu *et al*, where Equation 15 originated. This paper states that

$$A = W'(l_0) - W'(l_1) \tag{26}$$

where $W(x)$ is the shape function along the cantilever, l_o and l_1 represent the fixed and free ends, respectively. In the language of this project, $W(x)$ is the deflection as a function of x. Therefore, according to Equation 2, $W'(x)$ must be the derivative of $u(x)$ with respect to x, also known as the $\theta(x)$, the angle of deflection. At the fixed end, the angle of deflection is zero, so Equation 26 reduces to

$$A = -W'(l_1) = -\theta(L) = \frac{PL^2}{2EI} \tag{27}$$

Although it has been proven that A is not the maximum displacement, it can be seen that they are closely related

$$u(L) = \frac{PL^3}{3EI} \tag{28}$$

Consequently, utilizing the maximum displacement as A in Equation 15 will still provide a reasonably accurate analysis in terms of general design optimization trends, even if the numbers are not correct. Nonetheless, this paper has identified the error and made the proper adjustments to achieve accurate results and calculations.

Moment of Inertia

The theoretical model developed for the genetic algorithm optimization code makes the simplifying assumption that the bender consists of a single material. As a result, Equation 29 is used to evaluate the approximate moment of inertia.

$$I_{approx} = \frac{b(h+2t)^3}{12} \tag{29}$$

In reality, this assumption is not true as the piezoelectric layers and metal shim are characterized by different constants of elasticity, therefore altering the overall moment of inertia. However, this model has assumed that these differences are minimal, since the piezoelectric layer thickness is much less than the shim thickness. To validate this assumption, *Roundy and Wright* provide an expression for the effective moment of inertia for a composite beam, given in

Equation 30. The variables c_{sh} and c_p represent the elastic constants for the shim and piezoelectric material, respectively.

$$I_{eff} = 2\left[\frac{bt^3}{12} + bt\left(\frac{h+t}{2}\right)^2\right] + \frac{c_{sh}bh^3}{12c_p} \tag{30}$$

Table 7 provides a comparison of each method for calculating the moment of inertia. This comparison clearly shows that the approximate method is nearly identical to the method recommended by *Roundy and Wright*. As a result, it is conclusive that the approximation used to determine the moment of inertia does not contribute to the overall error of the theoretical model.

Table 7: Comparison of approximate and actual methods for calculating the moment of inertia for a composite beam. Note the difference is negligible.

I_{approx}	I_{eff}	$I_{approx} - I_{eff}$
$1.4400 \times 10^{-13} m^4$	$1.4400 \times 10^{-13} m^4$	$2.5244 \times 10^{-29} m^4$

Proof Mass Materials

The material chosen for the proof mass has a significant effect on the optimized design. A material with greater density will produce more output energy, according to Equation 16. Additionally, a denser material allows for smaller proof mass dimensions, thereby alleviating the area and volume constraints. For this reason, every simulation and calculation presented in this paper utilizes Tungsten. Tungsten is extremely dense (19250 kg/m^3) yet also widely available. However, it is much more expensive than the ABS plastic suggested in the project description. Clearly, ABS plastic is too light to optimize a model of reasonable size.

Alternative materials with high densities may also be investigated for energy harvesting applications. Gold, plutonium, platinum, and iridium are all extremely dense materials but rare and very expensive. Therefore, they are not recommended. An investigation of alloys may prove useful for finding cheap, dense materials as well. However, this is beyond the scope of this project and therefore left as further considerations for energy harvesting designs.

Energy Density

A general goal of all energy harvesters is to provide an output power density greater than that of tradition batteries. This is particularly useful for wireless sensors in which size and ease of maintenance are of highest priority. Roundy asserts that piezoelectric energy harvesters are capable of producing 0.5 to 100mW/cm^3. However, Designs #1 and #2 produce only about 0.066 mW/cm^3. It must be noted that most other designs only produce power on the order of micro-watts. A goal on 2.5mW is quite aggressive relative to previously proposed designs. As a result, space efficiency is sacrificed in order to achieve the design goals. Nonetheless, these designs provide plausible evidence towards optimizing "high-powered" energy harvesters.

Theoretical Analysis vs. FEA

As described in the results, the MATLAB program agrees very well with the hand-derived calculations. The genetic algorithm also agrees reasonably well with FEA for frequency, stress, and displacement analyses. The results from both the theoretically driven genetic algorithm and finite element analyses are provided in Tables 7 and 8. Both methods provide results that do not deviate by more than 25%. Therefore the simplified analytical model and alternative finite element simulation methods must be indicative of the actual energy harvesting system.

Table 8: GA and FEM Results Comparison for Design #1 with Percentage Difference.

Design #1	GA	FEM	% Difference
Natural Frequency	100.0673 Hz	89.215 Hz	-10.8 %
Maximum Stress	5.7031 MPa	4.348 MPa	-23.8 %
Maximum Displacement	4.9581 μm	5.577 μm	+12.5 %
Maximum Angle of Displacement	-0.0315°	-0.0351°	+11.4 %
Theoretical Power Output	3.29183 mW	3.6459 mW	+10.8 %

Table 9: GA and FEM Results Comparison for Design #2 with Percentage Difference.

Design #2	GA	FEM	% Difference
Natural Frequency	100.8855 Hz	92.029 Hz	-8.8 %
Maximum Stress	3.5239 MPa	2.712 MPa	-23.0 %
Maximum Displacement	4.878 μm	5.461 μm	+12.0 %
Maximum Angle of Displacement	-0.0246°	-0.0275°	+11.8 %
Theoretical Power Output	2.5 mW	2.861 mW	+14.4 %

There are many notable differences between the theoretically derived optimization algorithm and the finite element analysis. First, the theoretical method assumes the beam to be composed of a single one-dimensional material. However, finite element analysis is able to easily create composite beams of a specified thickness in which strain gradients occur across the y-direction. The theoretical model also assumes that the proof mass imparts a single concentrated force exactly at the end of the beam. In reality the proof mass distributes its weight across the beam. However, using a proof mass of lesser dimensions and greater density has reduced this effect. Another important difference between the two methods is that the analytical model assumes the total stress is dominated by the bending stress only. In reality shear stresses also play a role. However, the FEA has confirmed that bending stress does dominate total stress as represented by the Von Mises criteria. For additional quantifiable verification of the error between the two methods, refer to Table 5 above. For all cases the error difference never exceeds ±25%, a reasonably accurate result considering the simplified model and altered FEM model.

It should be noted that the FEM analyses were performed with the default tetrahedral global mesh size of 0.844 mm for Design #1 and 1.02 mm for Design #2. These values represented the maximum size able to accurately mesh the smallest feature of the device (piezoelectric layer). As a result, control meshes and/or finer meshes are unnecessary as the default sizes prove to be more than adequate.

Actual Design vs. Alternative FEM Design

The use of a proof mass design with 4mm x 4mm cross-section and greater mass density clearly cannot accurate simulate the actual design. However, it is possible to understand what characteristics the actual design may have by identifying trends. For example, consider proof masses of cross-sectional sizees 8mm x 8mm and 12mm x 12mm, shown below. For Design #1, this proof mass requires a mass density of 8.0641 x 10^5 kg/m^3 and 3.5840 x 10^5 kg/m^3 respectively to produce the same weight as the actual proof mass design.

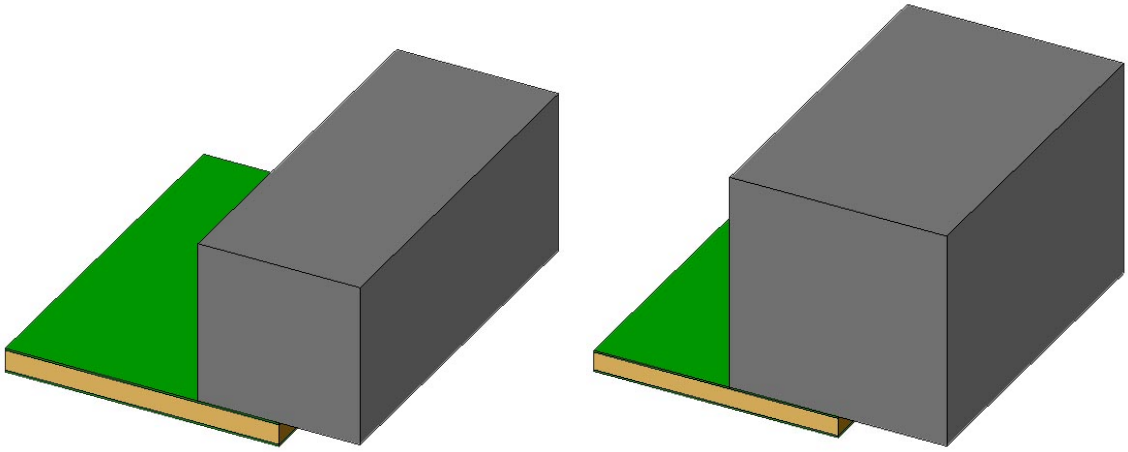

(a) (b)

Figure 13: Variations of alternative proof mass designs. Analysis of these models is performed on Design #1 to understand the behavior of the actual design. Figures (a) and (b) are 8mm x 8mm and 12mm x12mm cross-sections, respectively.

The same finite element analysis performed on Design #1 is done on these variations and summarized in Table 10. These general results show that as the proof mass increases, the natural frequency decreases. It is then reasonable to assume that the actual proof mass produces a natural frequency well out of the target range of 100 to 200 Hz and further away from the theoretical value. The stress appears to decrease away from the theoretical value as well. However, this result is favorable. The maximum displacement appears to decease and approach the theoretical value.

Table 10: FEM results of variations of the alternative design. Trends in proof mass size can be identified and extrapolated to understand the behavior of the actual proof mass.

FEM Result	4mm x 4mm	8mm x 8mm	12mm x 12mm
Natural Frequency	89.215 Hz	81.936 Hz	76.172 Hz
Maximum Stress	4.348 MPa	4.251 MPa	4.019 MPa
Maximum Displacement	5.577 μm	5.432 μm	5.096 μm

Although reasonably precise for small sized proof masses, the proposed analytical equations fail to be accurate when the proof mass is large compared to the bender. The governing equations for Bernoulli-Euler beam are only valid when the beam length is greater than ten times the beam width. For large proof masses this condition is not valid and therefore alternative theories must be pursued. A possible solution may be to apply a thin high-strength support to connect the proof mass to the free end. This will concentrate the weight at one point and more accurately represent a theoretical Bernoulli-Euler beam.

Alternative Designs

Although a simple cantilever beam is analyzed in this project, alternative geometries and more complicated designs can be pursued. For example, the design analyzed here utilizes a rectangular cantilever beam in which strain distributions are uneven for a given load. This fact is hidden from our simplified analysis, but nevertheless prevalent in the FEA. To alleviate this problem Baker *et al* suggests using a trapezoidal geometry designed to even the strain distribution throughout the system to achieve a claimed 30% increase in power output per volume. Additional modifications recommended by Baker *et al* seek to alleviate the frequency constraints and improve the coupling coefficients [3].

A more detailed analysis of piezoelectric coupling coefficients may reveal alternative methods for generating power. For this project, the d_{31} mode is utilized, however Jeon *et al* proposes that the d_{33} mode can generate 20 times higher voltage for equivalent geometries. The higher voltage produced will help overcome the forward bias of any diodes used in the rectifying electrical system [4].

Summary Conclusions

Basic Euler-Bernoulli beam bending analysis and a simplified model by Lu *et al* provide the theory used to develop a genetic algorithm for optimization of an energy harvester design. Through this analysis, two designs are proposed. The first design maximizes output power to produce 3.29183 mW at a natural frequency of 100.1 Hz and total volume of 49,995 mm^3. The second design minimizes total volume of the device to produce 2.5 mW at a natural frequency of 100.9 Hz and total volume of 38,281 mm^3. Both designs meet all engineering constraints and can be utilized for different applications. These results are validated to a certain degree with finite element analysis. Although all calculations agree to within ±25%, recommendations have been made to create theoretical models and designs that more accurately agree. Nonetheless, this paper proves useful in identifying trends and accurate design solutions for optimization of an energy harvester.

References

[1] Roundy S and Wright P K. "A piezoelectric vibration based generator for wireless electronics." Smart Mater, Stuct. 13 (2004) 1131-1142.

[2] Lu F, Lee H P, Lim S P. "Modeling and analysis of micro piezoelectric power generators for micro-electromechanical-systems applications." Smart Mater, Struct. 13(2004) 57-63.

[3] Baker J, Roundy S, Wright P K. "Alternative geometries for increasing power density in vibration energy scavenging for wireless sensor networks." Collection of Technical Papers – 3rd International Energy Conversion Engineering Conference (2005). v 2: 959-970.

[4] Jeon Y B, Sood R, Jeong J H, Kim S G. "Sensors and Actuators, A: Physical" (2006). v 122: 16-22.

Appendix

Nomenclature

a	Acceleration of vibration source, [m/s^2]
A	Maximum angle of displacement, [rad]
b	Width of beam, [m]
E	Elastic modulus of metal shim, [Pa]
e_{31}	Piezoelectric constant, [C/m^2]
f	Natural frequency of device, [Hz]
h	Thickness of metal shim, [m]
I	Moment of Inertia, [m^4]
L	Length of beam, [m]
l_0	Position at fixed end, [m]
l_1	Position at free end, [m]
M	Moment, [N-m]
P	Concentrated load, [N]
R	Matching resistance, [Ω]
t	Thickness of piezoelectric layer, [m]
u	Vertical displacement of beam, [m]
W	Shape function along the cantilever beam, [m]
x_m	Length of proof mass, [m]
y_m	Height of proof mass, [m]
z_m	Width of proof mass, [m]
ε_{33}	Relative permittivity of piezoelectric material, [F/m]
θ	Angle of Displacement, [rad]
ρ	Density of proof mass material, [kg/m^3]
σ	Maximum stress, [Pa]
ω	Natural angular frequency, [rad/s]

```
%% Project #3 - Design of an Energy Harvester
% Scott Moura
% SID 15905638
% ME 128, Prof. Lin

%% Genetic Algorithm
clear
tic;

% Define Constants (SI Units)
g = 9.8;        % Acceleration due to gravity
a = 0.2*g;      % Acceleration of Vibration Source
E_11 = 6.3e10;  % Elastic Modulus of the piezoelectric material
E = 11.7e10;    % Elastic Modulus of copper metal shim
rho_m = 19250;  % Density of end mass material

% Define constraints
volume_max = 50000 * (1/1000)^3;
area_top_max = 2500 * (1/1000)^2;
power_min = 2.5e-3;
sigma_max = 25e6;

% Constraint Counters
CC = zeros(5,1);

% Define Boundary Limits
L_min = 5e-3;
L_max = 25e-3;
b_min = 5e-3;
b_max = 50e-3;
t_min = 0.1e-3;
t_max = 0.1e-3;
h_min = 1e-3;
h_max = 1e-3;
x_m_min = 10e-3;
% x_m_max = 50e-3;
y_m_min = 10e-3;
y_m_max = 75e-3;
z_m_min = 10e-3;
z_m_max = 100e-3;

% Genetic Algorithm Parameters
d = 100;            % Number of Strings
iters = 100;        % Number of Generations/Iterations
start_pops = 100;   % Number of Starting Populations
nps = 10;           % Number of Parents to keep

% Displacement vs. Angle of Deflection
u_vec = zeros(d*iters*start_pops,1);
theta_vec = zeros(d*iters*start_pops,1);
aa = 1;

% Loop through each starting population
for idx1 = 1:start_pops

    % Define set of random strings
    Lambda = zeros(d,7);
```

```
    random = rand(d,7);
    Lambda(:,1) = L_min + random(:,1) * (L_max - L_min);              % L
    Lambda(:,2) = b_min + random(:,2) * (b_max - b_min);              % b
    Lambda(:,3) = t_min + random(:,3) * (t_max - t_min);              % t
    Lambda(:,4) = h_min + random(:,4) * (h_max - h_min);              % h
    Lambda(:,5) = x_m_min + random(:,5) .* (Lambda(:,1)*2 - x_m_min); % x_m
    Lambda(:,6) = y_m_min + random(:,6) * (y_m_max - y_m_min);        % y_m
    Lambda(:,7) = z_m_min + random(:,7) * (z_m_max - z_m_min);        % z_m

    % Repeat Genetic Algorithm for 50 iterations
    for idx2 = 1:iters

        % Initialization
        Pi = zeros(d,1);

        % Loop through each string
        for idx3 = 1:d

            % Parse out design variables
            L = Lambda(idx3,1);
            b = Lambda(idx3,2);
            t = Lambda(idx3,3);
            h = Lambda(idx3,4);
            x_m = Lambda(idx3,5);
            y_m = Lambda(idx3,6);
            z_m = Lambda(idx3,7);

            % Calc Design Variable-dependent parameters
            I = b*(h+2*t)^3/12;                 % Moment of Inertia
            m = rho_m * x_m * y_m * z_m;        % Mass of end mass
            P = m*a;                            % Force at end of beam
            u = (P*L^3)/(3*E*I);                % Max deflection
            A = -(P*L^2)/(2*E*I);               % Max angle of deflection
            omega = sqrt(a/u);                  % Natural freq of system
            M = P*L;                            % Moment at Fixed End
            sigma = M*(h/2 + t) / I;            % Stress at fixed end
            power = calcpower(A,omega,L,t,h,b); % Power output

            % Calculate top view area
            if b > z_m
                area_top = (L + 0.5*x_m) * b;
            else
                area_top = (L + 0.5*x_m) * z_m;
            end

            % Calcualte volume
            volume = area_top * (2*u + y_m);

            % Displacement vs. Angle of Deflection
            u_vec(aa) = u;
            theta_vec(aa) = A;
            aa = aa+1;

            % Calcualte the objective function, Pi
            %Pi(idx3) = 1/power;
            Pi(idx3) = volume;
```

```
            % Check Top View Area Constraint
            if (area_top > area_top_max)
                Pi(idx3) = inf;
                CC(1) = CC(1) + 1;
            end

            % Check Volume Constraint
            if (volume > volume_max)
                Pi(idx3) = inf;
                CC(2) = CC(2) + 1;
            end

            % Check Power Constraint
            if (power < power_min)
                Pi(idx3) = inf;
                CC(3) = CC(3) + 1;
            end

            % Check Maximum Stress
            if (sigma > sigma_max)
                Pi(idx3) = inf;
                CC(4) = CC(4) + 1;
            end

            % Check Natural Frequency
            f = omega / (2*pi);
            if (100 > f || f > 200)
                Pi(idx3) = inf;
                CC(5) = CC(5) + 1;
            end

        end

        % Rank the Genetic Strings output by Pi and save the best
        [sorted_Pi, order_Pi] = sort(Pi);
        if (sorted_Pi(10) == inf)
            %disp('INFINITY')
        end
        best1(idx2,idx1) = sorted_Pi(1);

        % Keep the Best Parents
        for i = 1:nps
            parent(i,:) = Lambda(order_Pi(i),:);
        end

        % Mate the Top Ten Parents to Generate Ten Children
        random2 = rand(nps,1);
        for j = 1:2:nps-1
            child(j,:) = random2(j,1) * parent(j,:) + (1 - random2(j,1)) * parent(j+1,:);
            child(j+1,:) = random2(j+1,1) * parent(j,:) + (1 - random2(j+1,1)) * parent(j ↙
+1,:);
        end

        % Generate New Random Strings to Combine with Parents and Children
        clear Lambda_new
        random3 = rand(d-2*nps, 7);
```

```
        Lambda_newrand(:,1) = L_min + random3(:,1) * (L_max - L_min);        % new L
        Lambda_newrand(:,2) = b_min + random3(:,2) * (b_max - b_min);        % new b
        Lambda_newrand(:,3) = t_min + random3(:,3) * (t_max - t_min);        % new t
        Lambda_newrand(:,4) = h_min + random3(:,4) * (h_max - h_min);        % new h
        Lambda_newrand(:,5) = x_m_min + random3(:,5) .* (Lambda_newrand(:,1)*2 - x_m_min) ↙
;  % new x_m
        Lambda_newrand(:,6) = y_m_min + random3(:,6) * (y_m_max - y_m_min);  % new y_m
        Lambda_newrand(:,7) = z_m_min + random3(:,7) * (z_m_max - z_m_min);  % new z_m

        Lambda_new = vertcat(parent, child, Lambda_newrand);

        % Repeat Genetic Algorithm
        Lambda = Lambda_new;

    end

    % Save the best lambda values
    Lambda_final(idx1,:) = Lambda(1,:);

end

% Output the design variable values for top five
best2 = best1(iters,:);
[sorted_best2, order_best2] = sort(best2);
for k = 1:5
    best_Lambda(k,:) = Lambda_final(order_best2(k),:);
    fprintf('Rank: %2.0f   L = %6.3fmm   b = %6.3fmm   t = %6.3fmm   h = %6.3fmm   x_m =  ↙
%6.3fmm   y_m = %6.3fmm   z_m = %6.3fmm  Volume = %5.0fmm^3\n',...
        k,best_Lambda(k,1)*1000,best_Lambda(k,2)*1000,best_Lambda(k,3)*1000,best_Lambda(k ↙
,4)*1000,...
        best_Lambda(k,5)*1000,best_Lambda(k,6)*1000,best_Lambda(k,7)*1000,sorted_best2(k) ↙
*1000^3);
end
disp(CC')
time = toc;
fprintf('Time: %5.4f sec\n',time)
disp(' ')
%plot(u_vec,theta_vec,'.')
```

```
function P = calcpower(A,omega,L,t,h,b)

% CALCPOWER
%   Determines the average power output by the energy harvester.
%   P = CALCPOWER(A,omega,L,t,h,b)
%   A     : strain at fixed end
%   omega : natural frequency
%   L     : length
%   t     : thickness of piezoelectric material
%   h     : thickness of metal shim
%   b     : width of beam
%   P     : Power

% Fixed values
e_31 = 250;
epsilon_33 = 3500*8.85e-12;

% Determine resistance for maximum power
R = t / (b*L*epsilon_33*omega);

% Calculate power
P = (omega^2*b^2*h^2*e_31^2*A^2) / (4 * (1 + b*L*epsilon_33*omega*R/t)^2) * R;
```

```
function props = ehprops(L,b,t,h,x_m,y_m,z_m)

% EHPROPS
%   Returns the properties of the energy harvester.
%   props = EHPROPS(L,b,t,h,x_m,y_m,z_m)
%   L   : Length of beam
%   t   : thickness of piezoelectric material
%   h   : thickness of metal shim
%   x_m : length of proof mass
%   y_m : height of proof mass
%   z_m : depth of proof mass

% Define Constants (SI Units)
g = 9.8;        % Acceleration due to gravity
a = 0.2*g;      % Acceleration of Vibration Source
E = 11.7e10;    % Elastic Modulus of the copper shim
E_11 = 6.3e10;  % Elastic Modulus of the piezoelectric material
rho_m = 19250;  % Density of plastic end mass material
e_31 = 250;     % Piezoelectric constant
epsilon_33 = 3500*8.85e-12; % Permittivity

% Calc Design Variable-dependent parameters
I = b*(h+2*t)^3/12;                 % Moment of Inertia
m = rho_m * x_m * y_m * z_m;        % Mass of end mass
P = m*a;                            % Force at end of beam
u = (P*L^3)/(3*E*I);                % Max deflection
A = -(P*L^2)/(2*E*I);               % Max angle of deflection
omega = sqrt(a/u);                  % Natural angular freq of system
f = omega / (2*pi);                 % Natural freq of system
M = P*L;                            % Moment at Fixed End
sigma = M*(h/2 + t) / I;            % Stress at fixed end
power = calcpower(A,omega,L,t,h,b); % Power output
R = t / (b*L*epsilon_33*omega);     % Resistance for maximum power
area_top = (L + 0.5*x_m) * z_m;     % Area from top-view
volume = area_top * (2*u + y_m);    % Total volume of device


% Output Properties
props.power = power;
props.area = area_top;
props.volume = volume;
props.disp = u;
props.theta = A;
props.stress = sigma;
props.afreq = omega;
props.nfreq = f;
props.maxresist = R;
```

```
function [f,P] = freqplot(L,b,t,h,x_m,y_m,z_m)

% Set range of frequencies
f = linspace(0,500,1000);
omega = 2*pi*f;

% Fixed values
e_31 = 250;
epsilon_33 = 3500*8.85e-12;

% Determine omega and A
props = ehprops(L,b,t,h,x_m,y_m,z_m);
A = props.theta;
R = props.maxresist;
fn = props.nfreq;
omega_n = 2*pi*fn;

% Calculate power
P = 1000 * (omega.^2*b^2*h^2*e_31^2*A^2) ./ (4 * (1 + b*L*epsilon_33*omega*R/t).^2) .* R;
Pn = 1000 * (omega_n^2*b^2*h^2*e_31^2*A^2) / (4 * (1 + b*L*epsilon_33*omega_n*R/t)^2) * R;
Pn1 = linspace(0,Pn,100);

% Plot
plot(f,P,'b',fn,Pn1,'r--',fn,Pn,'ro')
title('\bfOutput Power vs. Frequency')
xlabel('Frequency (Hz)')
ylabel('Power (mW)')
```

```
function [R,P] = rplot(L,b,t,h,x_m,y_m,z_m)

% Fixed values
e_31 = 250;
epsilon_33 = 3500*8.85e-12;

% Determine omega and A
props = ehprops(L,b,t,h,x_m,y_m,z_m);
A = props.theta;
omega = props.afreq;

% Set range of resistances
Rmax = t / (b*L*epsilon_33*omega);
R = linspace(0,10*Rmax,1000);

% Calculate power
P = 1000 * (omega^2*b^2*h^2*e_31^2*A^2) ./ (4 * (1 + b*L*epsilon_33*omega*R/t).^2) .* R;
Pmax = linspace(0,max(P),100);

% Plot
plot(R*1e-3,P,'b',Rmax*1e-3,Pmax,'r--',Rmax*1e-3,max(P),'ro')
title('\bfOutput Power vs. External Resistance')
xlabel('Resistance (k\Omega)')
ylabel('Power (mW)')
```

```
function [P,R,f] = rfreqplot(L,b,t,h,x_m,y_m,z_m)

% Fixed values
e_31 = 250;
epsilon_33 = 3500*8.85e-12;

% Determine omega and A
props = ehprops(L,b,t,h,x_m,y_m,z_m);
A = props.theta;
omega_n = props.afreq;

% Set range of resistances
Rmax = t / (b*L*epsilon_33*omega_n);
R = linspace(0,10*Rmax,50);

% Set range of frequencies
f = linspace(0,500,50);
omega = 2*pi*f;

% Initialize P matrix
P = zeros(50,50);

% Calculate power
for i = 1:length(omega)
    for j = 1:length(R)
        P(i,j) = 1000 * (omega(i)^2*b^2*h^2*e_31^2*A^2) / (4 * (1 + b*L*epsilon_33*omega( ↙
i)*R(j)/t)^2) * R(j);
    end
end

% Plot
surf(1e-3*R,f,P);
title('\bfOutput Power vs. Resistance & Frequency')
xlabel('Resistance (k\Omega)')
ylabel('Frequency (Hz)')
zlabel('Power (mW)')
```